

# Depth Prediction of Nanotags in Tissue Using Surface Enhanced Spatially Offset Raman Scattering (SESORS)

## *Electronic Supporting Information*

Matthew E. Berry, <sup>a</sup> Samantha M. McCabe, <sup>a</sup> Neil C. Shand, <sup>b</sup> Duncan Graham <sup>a</sup> and Karen Faulds <sup>\*a</sup>  
<sup>a</sup>*Centre for Molecular Nanometrology, Department of Pure and Applied Chemistry, University of Strathclyde,  
99 George Street, Glasgow, G1 1RD, United Kingdom.*  
<sup>b</sup>*DSTL, Porton Down, Salisbury, SP4 0JQ, United Kingdom.*

### Table of contents

Chemicals and reagents	S2
Figure S1. Spectroscopic and structural information for PPY and BPE	S2
Synthesis of SERS active NPs	S2
Characterisation of SERS active NPs	S2
Figure S2. Characterisation of SERS active NPs	S3
SESORS experimental setup	S3
Figure S3. Optical setup for SESORS experiments	S4
Data processing	S4
Equation 1. Root-mean-square error of calibration	S4
Figure S4. Principal component analysis for the tracking of nanotags through tissue	S5
Figure S5. Justification for the use of the natural logarithm of the intensity ratio	S5
References	S5

## Chemicals and reagents

Sodium tetrachloroaurate (III) dihydrate, trisodium citrate, 4-(1H-pyrazol-4-yl)pyridine (PPY), 1,2-bis(4-pyridyl)ethylene (BPE), methanol, (3-aminopropyl)triethoxysilane (APTES) and sodium silicate were purchased from Sigma Aldrich. Milli Q water (MQ H<sub>2</sub>O) was prepared in house. The Raman reporters, BPE and PPY, were prepared in stock solutions by dissolving the solid in methanol. Subsequent dilutions were then carried out in MQ H<sub>2</sub>O.

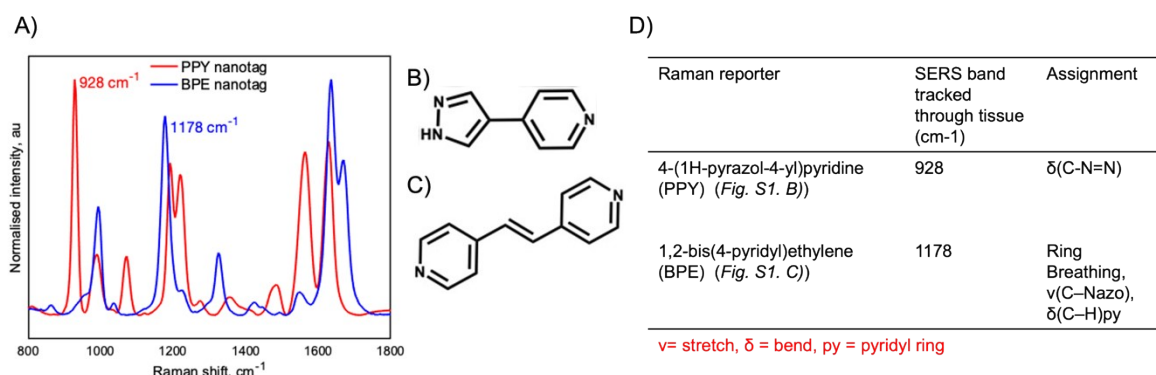


**Figure S1.** Spectroscopic and structural information for PPY and BPE. A) Truncated, baselined, and normalised SERS spectra of PPY (red) and BPE (blue) silica encapsulated AuNPs developed for this study. The SERS bands used to track the NPs through tissue barriers are highlighted. B) Chemical structure of the Raman reporter PPY. C) Chemical structure of the Raman reporter BPE. D) Table providing the assignments of the SERS bands used to track the NPs through tissue for both PPY and BPE.<sup>1</sup>

## Synthesis of SERS active NPs

Gold NP (AuNP) seeds with an average size of between 50 and 60 nm were synthesised using a modified Turkevich method where citrate ions act as the reducing and capping agent for the NPs.<sup>2</sup> Sodium tetrachloroaurate (III) dihydrate (70 mg) was added to MQ H<sub>2</sub>O (500 mL) and heated to boiling. Trisodium citrate (42 mg) was added to MQ H<sub>2</sub>O (7.5 mL), and the solution was combined with the boiling solution. The combined mixture was boiled for 15 minutes with continuous stirring and then allowed to cool.

SERS active silica coated AuNP aggregates were synthesised using a method modified from Li *et al.*<sup>3</sup> Raman reporters (300 μL, 100 μM) were added separately to a solution of AuNPs (100 mL) under stirring. The solution was stirred until the SERS response was optimised or the solution became noticeably darker in colour (3 to 5 minutes for BPE, 30 seconds to 1 minute for PPY because the colour change occurred quickly, and this is indicative of aggregation). APTES (1.6 μL, undiluted) was then added followed immediately by sodium silicate (111 μL, undiluted). The mixture was stirred vigorously at boiling for 30 minutes, and it was then removed from heat and stirred overnight. The NPs were then centrifuged (7300g, 20 mins) and resuspended in MQ H<sub>2</sub>O (30 mL).

## Characterisation of SERS active NPs

*Extinction spectroscopy:* A Cary 60 UV-Visible Spectrophotometer with a wavelength range of 300-900 nm and a scan rate of 600 nm/min was used for all extinction spectra, which were used to determine the size and stability of the SERS active nanotags. PPY nanotags (400 μL; dilution factor 4) and BPE

nanotags (400  $\mu\text{L}$ , dilution factor 5) were added to a poly(methyl methacrylate) (PMMA) cuvette for all measurements.

*Dynamic light scattering (DLS) and zeta potential:* A Malvern Zetasizer nano ZS system was used to conduct DLS and zeta potential measurements. PPY and BPE NPs were added to a PMMA cuvette for all measurements. For zeta potential measurements, a dip cell was placed into the cuvette.

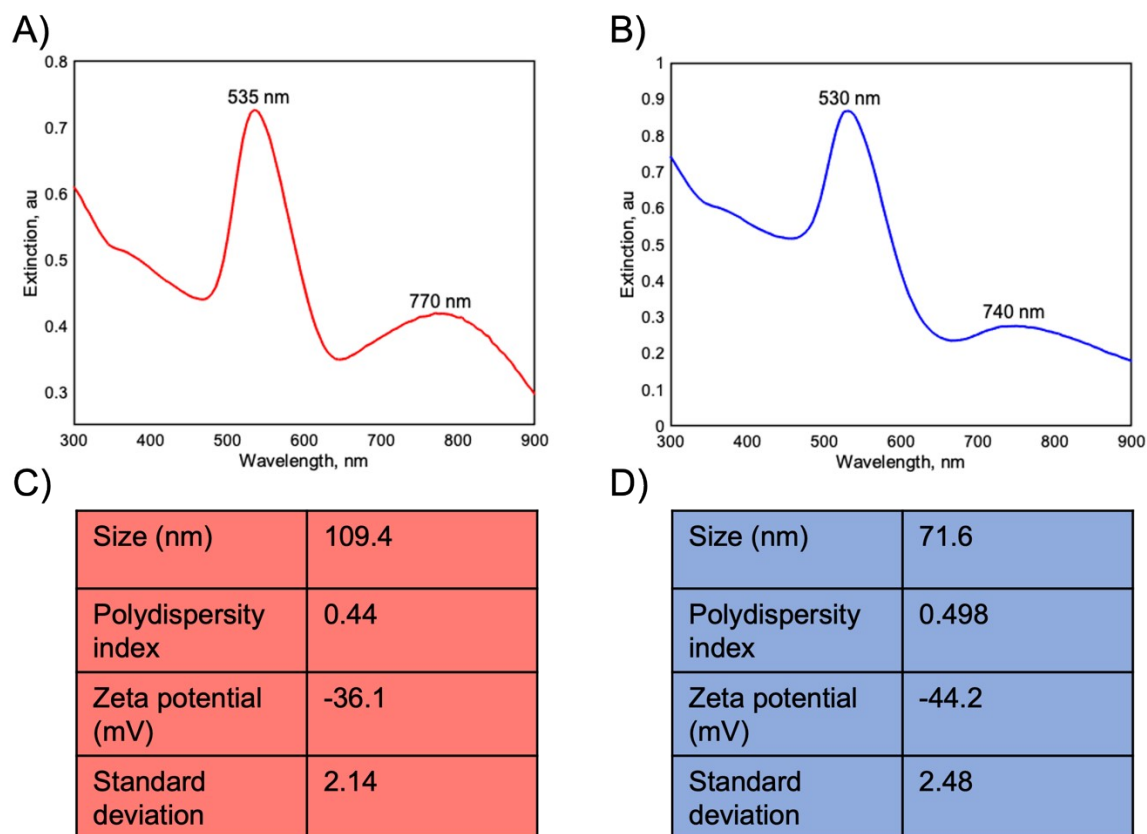


**Figure S3.** Characterisation of SERS active nanotags. A) Extinction spectrum for PPY nanotag. B) Extinction spectrum for BPE nanotag. C) DLS and zeta potential analyses for PPY nanotag. D) DLS and zeta potential analyses for BPE nanotag.

### SESORS experimental setup

For the SESORS experiments, SERS active NPs (1 mL, 87 pM (approximated to  $5.4 \times 10^{10}$  particles/mL) PPY; 274 pM (approximated to  $1.6 \times 10^{11}$  particles/mL) BPE) were first centrifuged and resuspended in MQ  $\text{H}_2\text{O}$  (350  $\mu\text{L}$ , 248 pM PPY; 782 pM BPE) before being pipetted into a quartz microcuvette, path length 5 mm, chamber volume 350  $\mu\text{L}^4$ . Pork tissue was obtained from a local supermarket and cut into sections (roughly 25 mm x 25 mm with 3 mm thickness). SESORS experiments were prepared by overlaying the cuvette with tissue sections and increasing the thickness in 3 mm increments up to a maximum barrier of 60 mm (20 layers). Measurements were taken using a handheld Resolve instrument from Cobalt Light Systems (830 nm, average laser power 450 mW). Measurements were carried out at each depth and for both references in triplicate using a 2 second integration time, 6 accumulations per measurement and an 8 mm offset. To use the instrument in a contact mode setting, a z-translational stage was used to bring the samples into contact with the nose cone of the spectrometer. The stage was manoeuvred until resistance was experienced when turning the stage handle.

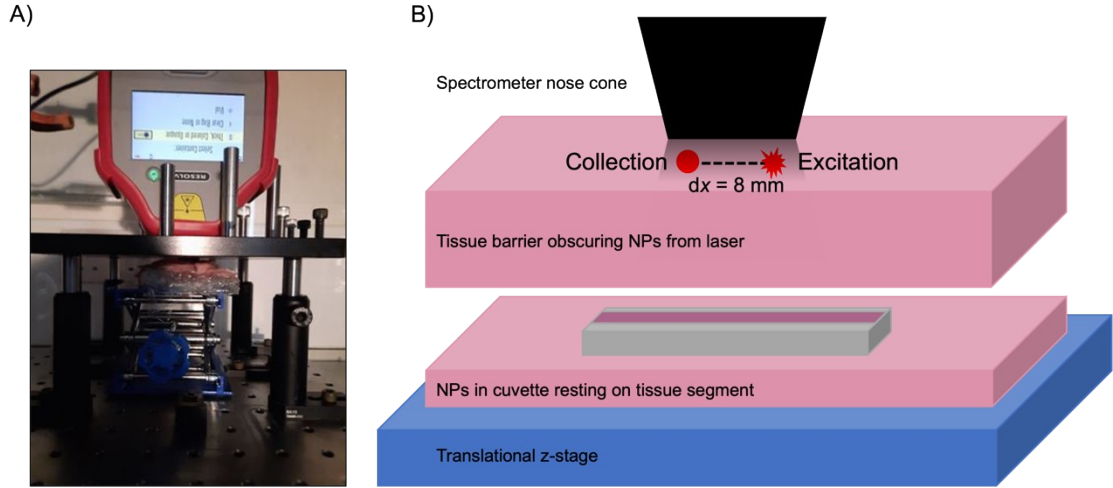


**Figure S3.** Optical setup for SESORS experiments. A) Photograph of the experimental setup using a handheld SORS spectrometer for the detection of SERS active nanotags through tissue. B) Schematic illustrating the various layers depicted in the photograph. Nanotags were held in a cuvette on a tissue segment resting on a translational z-stage. The cuvette was then overlaid with tissue barriers of varying thicknesses, and the multi-layered sample was brought into contact with the nose cone of the handheld SORS spectrometer by adjusting the stage until resistance was experienced when turning the handle to ensure no space between the sample and the instrument.

## Data processing

All spectra were processed using MATLAB software (Version 2018b, The MathWorks, Natick, MA, USA). Pre-processing involved truncating and baselining the spectra collected at an 8 mm offset through various tissue depths. For the SESORS plots in Figure 1, spectra were averaged, normalised, and stacked. Principal component analysis (PCA) was applied to analyse the data from the SESORS stack plots to establish the Raman bands with the highest variance across all offset spectra collected at each depth and the spectra corresponding to the NP and tissue references. The calibration plots were developed by plotting the truncated, baselined, and averaged offset spectra collected at each tissue depth and then recording the intensity of the NP ( $928\text{ cm}^{-1}$  for PPY and  $1178\text{ cm}^{-1}$  for BPE) and tissue ( $1444\text{ cm}^{-1}$ ) Raman bands. The natural logarithm of the NP/tissue ratio at each depth was then calculated and these values were plotted against the tissue depth. For depth prediction measurements, root-mean-square error of calibration (RMSEC) and RMSEC % was calculated for the predicted versus measured data sets. The formula used can be observed in Equation 1),

$$1) \quad RMSEC = \sqrt{\frac{1}{N_{sample} - 2} \sum_{i=1}^{N_{sample}} (\hat{x}_i - x_i)^2}$$

where  $N_{sample}$  is the number of observations in the calibration set,  $\hat{x}_i$  is the predicted value of the  $i$ th observation, and  $x_i$  is the measured value of the  $i$ th observation.<sup>5</sup> Note that  $N_{sample} - 2$  was used to reduce sample bias.

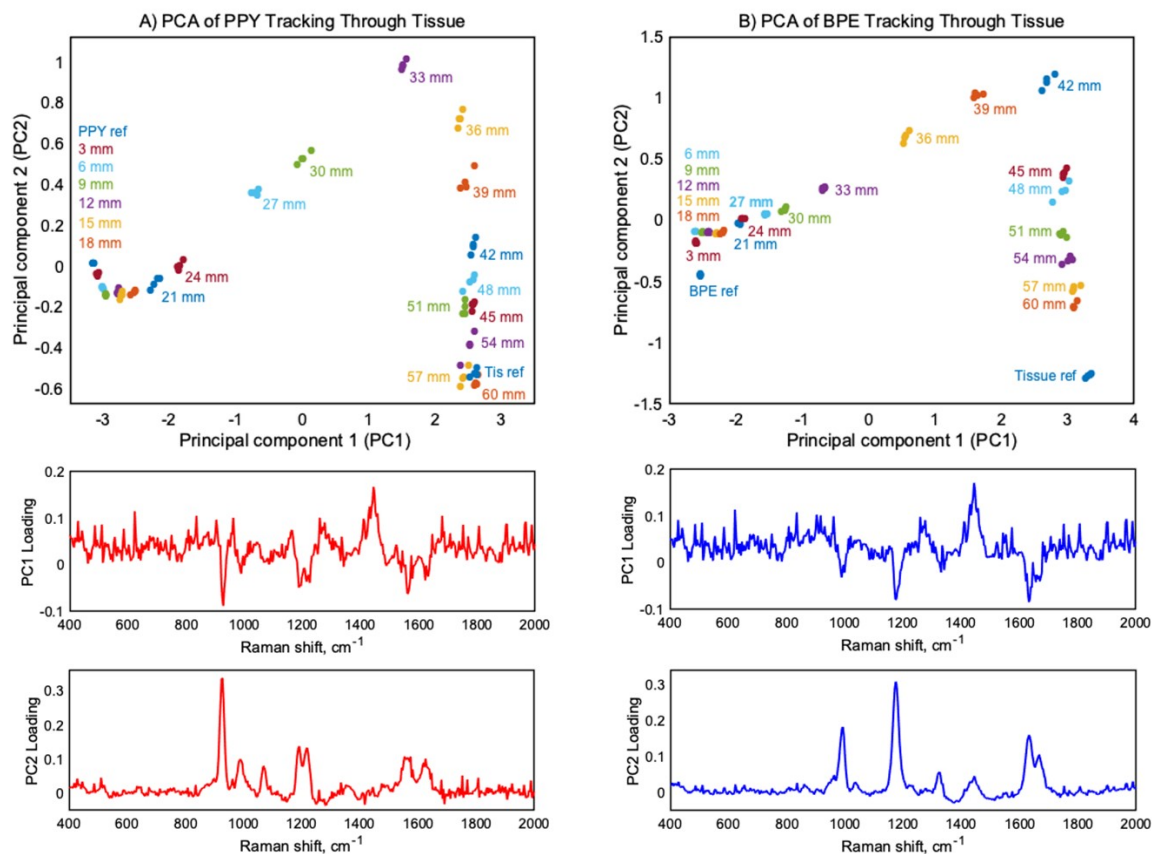


**Figure S4.** Principal component analysis (PCA) for the tracking of A) PPY and B) BPE nanotags through porcine tissue up to 60 mm. The PCA plots from SORS spectra of increasing tissue thicknesses with nanotag and tissue reference spectra show discrimination between tissue thicknesses up to depths of 42 mm for PPY and 48 mm for BPE in the first and second principal components. The spectra below show PC1 (top) and PC2 (bottom) loading plots indicating the Raman shifts at which the highest variance occurs across the experiment. Distinct separation can be observed between the nanotag and tissue spectra for both Raman reporters.

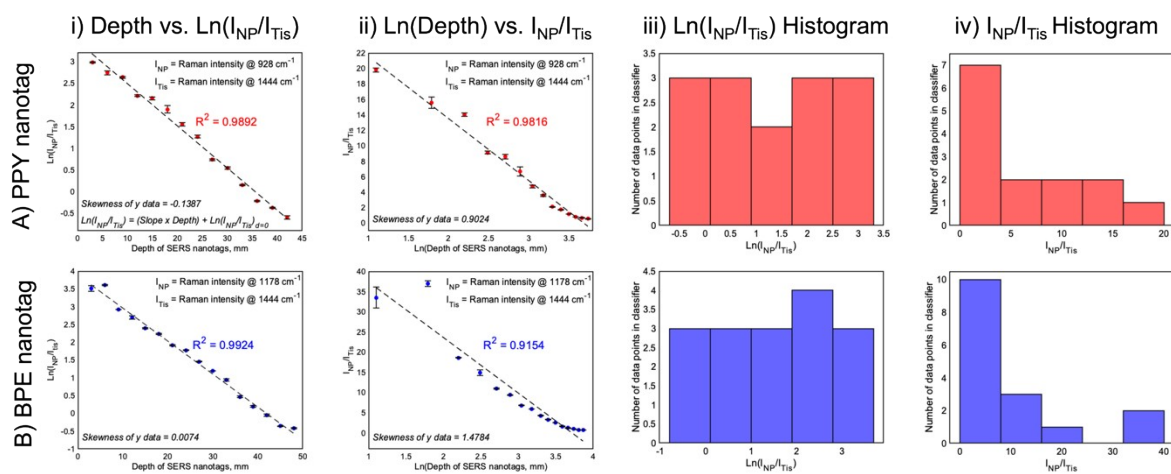


**Figure S5.** Justification for the use of the natural logarithm of the ratio of the nanotag versus tissue Raman intensities in the development of the depth calibration curves. A) Depth determination experiment using the PPY nanotag represented via i) a plot of the natural logarithm of the intensity ratio (the independent variable) versus the depth of the nanotag (the dependent variable) and ii) a plot of the pure intensity ratio versus the depth of the nanotag. iii) A histogram representing the distribution of the dataset of the natural logarithm of

the intensity ratio for the PPY nanotag. iv) A histogram representing the distribution of the dataset of the pure intensity ratio for the PPY nanotag. B) Depth determination experiment using the BPE nanotag represented via i) a plot of the natural logarithm of the intensity ratio versus the depth of the nanotags and ii) a plot of the pure intensity ratio versus the depth of the nanotag. iii) A histogram representing the distribution of the dataset of the natural logarithm of the intensity ratio for the BPE nanotag. iv) A histogram representing the distribution of the dataset of the pure intensity ratio for the BPE nanotag.

## References

- 1 H. Kearns, N. C. Shand, W. E. Smith, K. Faulds and D. Graham, *Phys. Chem. Chem. Phys.*, 2015, **17**, 1980–1986.
- 2 J. Turkevich, P. C. Stevenson and J. Hillier, *Discuss. Faraday Soc.*, 1951, **11**, 55–75.
- 3 J. F. Li, X. D. Tian, S. B. Li, J. R. Anema, Z. L. Yang, Y. Ding, Y. F. Wu, Y. M. Zeng, Q. Z. Chen, B. Ren, Z. L. Wang and Z. Q. Tian, *Nat. Protoc.*, 2013, **8**, 52–65.
- 4 W. Haiss, N. T. K. Thanh, J. Aveyard, and D. G. Fernig, *Anal. Chem.* **79**, 4215-4221.
- 5 W. da S. Lyra, L. F. de Almeida, F. A. da S. Cunha, P. H. G. D. Diniz, V. L. Martins and M. C. U. de Araujo, *Anal. Methods*, 2014, **6**, 1044–1050.